Microwave Parametric Transducers For The Next Generation Of Resonant-Mass Gravitational Wave Detectors

Michael E. Tobar
Department of Physics, the University of Western Australia, Nedlands, 6907 WA, Australia

Abstract

It is shown that a large improvement in liquid helium and ultra-cryogenically cooled resonant-mass gravitational wave detectors can be achieved through the use of low acoustic loss materials such as sapphire and niobium, and new low noise microwave technology. Applied to the liquid helium cooled UWA antenna, Niobe, a millisecond burst sensitivity of order 10^{-20} can be achieved, corresponding to a spectral strain sensitivity of $2\times10^{-22}/\sqrt{Hz}$ with a 50 Hz bandwidth. Applied to the proposed ultra-cryogenic spherical GRAIL detector in the Netherlands, a spectral strain sensitivity of better than $10^{-23}/\sqrt{Hz}$ with a bandwidth of order 100 Hz can be achieved, which is close to the quantum limit.

1. Introduction

Resonant-mass detectors world-wide currently operate at a frequency of about 1 kHz with a noise temperature of a few mK, corresponding to a millisecond burst strain sensitivity of order a few by 10^{-19}, or a spectral strain sensitivity of order $10^{-21}/\sqrt{Hz}$ with a 1 Hz bandwidth. However, these detectors are still many orders of magnitude away from the quantum limit given by $T_n \approx h\omega/k_B = 0.05\ \mu$K for a 1 kHz resonance. The need to improve this sensitivity is driven by theoretical calculations of expected gravitational wave sources. The chance of detecting gravitational wave bursts depends strongly on the efficiency at which mass is converted to gravitational radiation. The current generation of gravitational wave detectors are capable of detecting gravitational collapse events of 10^{-3} efficiency with a signal to noise ratio of 1 at a distance of 10 kiloparsecs. This is only likely to occur once every few decades. Clearly the detection of gravitational waves is unlikely among the current generation of resonant detectors. Sensitivity to detect 10^{-6} efficient events in our galaxy is the goal of laser interferometer detectors currently under construction (LIGO, VIRGO, GEO, TAMA), and of the ultra cryogenic bars and spherical detectors. These detectors are currently expected to be completed a few years after the year 2000.

The Niobe antenna at the University of Western Australia is currently a two-mode detector configured with a microwave superconducting re-entrant cavity transducer, which has been described in detail previously.[1] As an alternative, several years ago the sapphire transducer was proposed.[2] Since this time the concept has been tested[3,4] and new and improved oscillators developed.[5–8] As a consequence the potential exists to significantly improve the sensitivity of resonant-mass detectors. The antenna-transducer system presented here makes use of new low-noise microwave technology and the low electrical and acoustic losses in monocrystalline sapphire and niobium.[9] The sensitivity is analysed using a frequency domain technique from a lumped-mass model interacting with a capacity transducer. The calculations here suggest by imple-

menting the parametric transducer technology, a noise temperature of the order of a few μK can be achieved in a liquid helium cooled detector, and one tenth of a μK in a ultra-cryogenic detector. This noise temperature is equivalent to a millisecond burst sensitivity of order 10^{-20} and a few by 10^{-21} for the NIOBE detector respectively. For the proposed GRAIL detector this is equivalent to a millisecond burst sensitivity of order a few by 10^{-21} and a few by 10^{-22} respectively. The Grail detector will consist of a 117 tonne CuAl sphere cooled to about 15 mK. Quoted sensitivities are competitive with the large km scale interferometric detectors.

2. Frequency Domain Sensitivity Calculations

Detector sensitivity has been calculated[10,11] using standard frequency domain techniques described in detail in.[12] Calculations of the spectral density of the competing noise components are presented in the form of the spectral strain sensitivity/$\sqrt{Hz}$. From this, the burst sensitivity, h, noise temperature, T_n, and detector bandwidth, Δf_d, can be calculated by;

$$h = \frac{\Delta f_s}{2}\left(\int_0^\infty h^+(f)^{-2}\,df\right)^{-\frac{1}{2}} \tag{1}$$

$$\frac{8\,L\,{f_1}^4\,m_1}{k_B}\left(\int_0^\infty h^+(f)^{-2}\,df\right)^{-1} \tag{2}$$

$$\Delta f_d \approx h^+(f_{min})^2\int_0^\infty h^+(f)^{-2}\,df \tag{3}$$

where Δf_s is the burst signal bandwidth (1 kHz for a millisecond pulse), $h^+(f)$ is the single sided spectral strain sensitivity (the superscript, +, refers to single sided) , m_1 is the effective mass of the primary resonator, f_1 the bar resonant frequency, L the bar length, k_B Boltzmanns constant and f_{min} the frequency of minimum strain noise density. For a bar detector the effective mass is related to the physical mass by $m_1 = m_{bar}/2$, and for a spherical detector it is related by $m_1 = 6\chi m_{sphere}/5$, assuming a dodecahedral arrangement of 6 multi-mode displacement amplifiers and transducers around the sphere.[13,14] Here, χ is a factor that depends on the material properties of the sphere and is usually of the order 0.3. For the NIOBE bar, m_1 is 755 kg, and for the GRAIL sphere it is 42×10^3 kg.

The spectral strain sensitivity can be calculated from the individual noise components, for the model shown in figure 1, this is given by;[12]

$$h^+(f) = \frac{\sqrt{{S_{xn}}^+(f)}}{8\,f^2\,L\,m_1\,G_{n1}(f)}, where, {S_{xn}}^+(f) = {S_{xtot}}^+(f) + \sum_{j=1}^{n}{S_{Fj}}^+(f)\,|G_{nj}(f)| \tag{4}$$

Here, $G_{nj}(f)$ is the Fourier transform of the impulse response (or transfer function) of displacement sensed by the transducer per force input at the jth lumped element, $S^+_{Fj}(f)$ [N^2/Hz] is the spectral density of force on the jth lumped element and $S^+_{xtot}(f)$

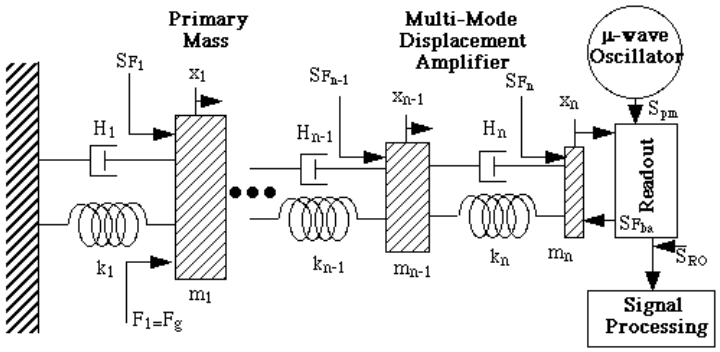

Figure 1: Schematic of a lumped mass model of a n-mode resonant-mass gravity wave detector with an electronic readout. The jth element has the following properties with respect to an infinite wall; effective mass m_j, spring constant k_j and dissipation constant H_j. Each resonant mass will be excited by a spectral density of force S_{Fj} [N^2/Hz] due to the finite temperature and dissipation, as well as back-action from the readout. The readout and pump oscillator also add a spectral density of electronic noise (S_{RO},S_{pm}), both can be normalised with respect to the displacement sensitivity of the readout and expressed in units of [m^2/Hz].

[m^2/Hz] is the sum of the contributions to the transducer electronic noise referred to a displacement at the final nth mode. (This includes the oscillator phase noise and read-out noise of the detection scheme)

For a spherical detector equations (1) and (3) still hold, however (2) and (4) have slightly different and more complicated forms.[13,14] For the Niobe detector we can combine (1) and (2) and derive the relation between the noise temperature and burst sensitivity. For a millisecond burst this has been calculated to be[12] $h_{1ms} = 5.5 \times 10^{-19}\sqrt{Tn}$, and for the Grail detector a similar relation may be derived which gives, $h_{1ms} = 4.4 \times 10^{-20}\sqrt{Tn}$. In a similar way, one may define an effective length of the sphere and then still make use of (2) and (4).

3. Parametric Transducer Narrow-Band Noise Components

Narrow-band noise components may be characterised by the spectral density of force that excites the resonant system. For a parametric system the two major noise components are due to the fluctuations arising from the back action effect of S_{am} of the pump oscillator, and the Nyquist fluctuations due to the finite temperature and acoustic Q of the resonant detector.

Assuming that the electrical transducer is impedance matched the force fluctuations incident on the final resonant mass, m_n, due to S_{am} are given by;

$$S_{Fam}(f) = \frac{{P_{inc}}^2}{2\,{\Omega_0}^2}\left(\frac{2\,Q_e}{f_0}\frac{df}{dx}\right)^2 S_{am}\ [N^2/Hz] \qquad (5)$$

Here, $\Omega_0 = 2\pi f_0$ is the transducer electrical frequency, which is 9.5 GHz for the

re-entrant cavity transducer.

The Nyquist noise driving the ith lumped element in the resonant detector is given by;

$$S_{Fnyq\,i}(f) = 4\,k_B\,m_i\,\omega_i\frac{T}{Q_i}\;[N^2/Hz] \tag{6}$$

For the present system operating on Niobe, the pump oscillator driving the transducer is limited by the AM noise of a typical microwave amplifier (S_{am} ≈-140 dBc/Hz). Typically the transducer operates with a P_{inc} of 10 μW. In this case, from (5), the amplitude noise creates a back-action force density of order 5×10^{-27} N^2/Hz, while the Nyquist component at 5 K for the Nb secondary mass (Q≈10^7) was calculated from (6) to be 5×10^{-26} N^2/Hz.

4. Parametric Transducer Broad-Band Noise Components

Broad-band noise components may be characterised by the spectral density of displacement referred to motion of the nth lumped element sensed by the transducer. The two major noise components arise from the phase fluctuations of the incident pump oscillator, and the noise temperature of the first microwave amplifier in the readout chain, $T_{amp}(f)$.

The power in the signal sidebands is proportional to $P_{inc}Q_e^2(df/dx)^2$, which means that the noise due to the readout system effective noise temperature is proportional to the inverse of this quantity. For an impedance matched transducer this quantity is given by;

$$S_{RO}(f) = \frac{T_{amp}(f)\,k_B}{P_{inc}}\left(\frac{2\,Q_e}{f_0}\frac{df}{dx}\right)^{-2}\;[m^2/Hz] \tag{7}$$

Thus, by increasing P_{inc} and Q_e(df/dx) the broad band noise due to S_{RO} will be reduced at the expense of enhanced narrow band noise due to back-action caused by S_{am}. In addition, S_{pm} adds to the broad band noise. However, this component of broad band noise is independent of P_{inc}, because the ratio of the signal sidebands to the reflected noise power remains constant, and is given by;

$$S_x(f) = \left(\frac{df}{dx}\right)^{-2} f^2 S_{pm}(f)\;[m^2/Hz] \tag{8}$$

This noise term can only be reduced by increasing df/dx or reducing S_{pm}.

Existing tunable microwave pump oscillators have a S_{pm} of -145 dBc/Hz.[15] From (8), this is equivalent to a displacement sensitivity of 1.3×10^{-19} m/$\sqrt{Hz}$. For Niobe, the broad band noise is due to T_{amp} and has been measured to be 3×10^{-17} m/$\sqrt{Hz}$. From (7), the effective noise temperature of the amplifier can be calculated to be 2.6×10^4 K. This large noise temperature is because the read out amplifier exhibits flicker noise even at low input powers of order of a nano Watt.

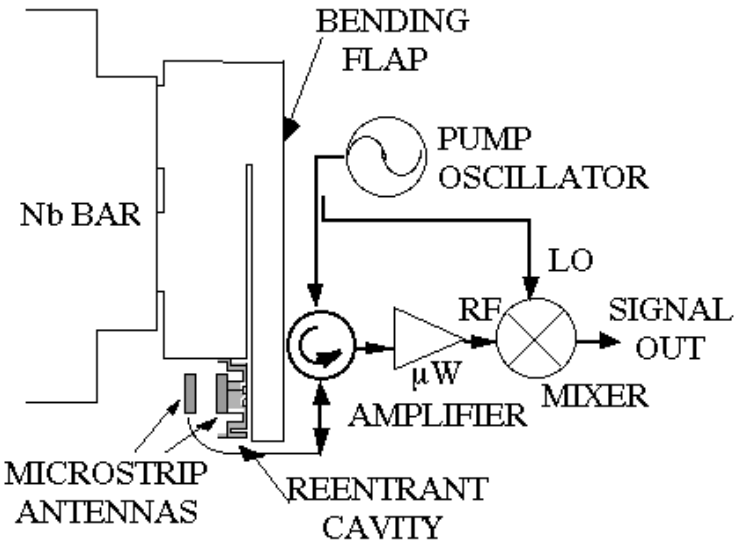

Figure 2: Schematic of the current re-entrant cavity transducer attached to Niobe. The transducer is non-contacting, microwaves are transported to the transducer via radiation between two microstrip antennas. This is very important for the vibration isolation perspective.

5. Re-entrant Cavity Transducer

A schematic of the current re-entrant cavity transducer attached to Niobe is shown in figure 2. The transducer consists of a superconducting microwave re-entrant cavity resonator glued to the base of a bending flap secondary resonant-mass, which is tuned to the resonant frequency of the bar. The gap spacing is about 15 μm and has a displacement sensitivity of df/dx=3×10^{14} Hz/m and an electrical quality factor of 10^5.

6. Sapphire Dielectric Transducer

The sapphire transducer consists of a single piece of low-loss sapphire crystal which acts as both the acoustic oscillator and the dielectric transducer. It has been shown to have a displacement sensitivity of df/dx = 2×10^{12} Hz/m and electrical quality factor of greater than 2×10^8. However, with optimisation of the dimensions as shown in figure 3, it is possible that a df/dx of 8-9$\times10^{12}$ Hz/m can be obtained.[16] Also, in principle the electrical Q-factor of such a device can be greater than 10^9 if care is taken to avoid contamination.[17] Sapphire also exhibits a high acoustic Q-factor, values of greater than 10^9 have been measured at 4 K.[9] A schematic of the transducer attached to Niobe is shown in figure 3. The proposed antenna is a three-mode device with a niobium intermediate mass. The transducer consists of a simple non-contacting design consisting of two microstrip patch antennas which radiate microwaves through an air gap. This is advantageous as there is no need to vibrationally isolate any cables connected to the transducer.[18]

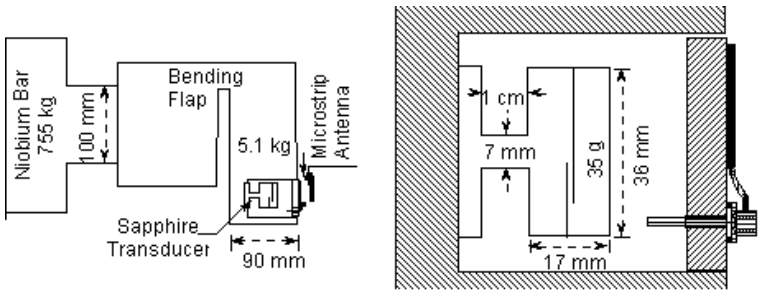

Figure 3: Schematic of the two-mode sapphire transducer for Niobe (three-mode detector). The fundamental clapping mode of the slotted sapphire can be tuned to the Nb bar at 710 Hz.

7. Comparison of the Dielectric and Re-entrant Transducers at 4 K

The lowering of the pump oscillator noise will enable an increase in incident power, P_{inc}, improving the noise floor due to the displacement noise of the readout given by (7), without degrading S_{Fam} caused by the oscillator amplitude fluctuations given by (5). However, because the re-entrant cavity transducer quality factor degrades for input powers above a few tens of μW, the displacement sensitivity does not improve significantly with an increase in microwave power. It has been found that the current operating condition of 10 μW is optimum . Also, a prototype sapphire transducer has consistently been operated cooled to 4.2 K with an input power of order 10 mW. However, because the back-action degrades with input power squared, it is prudent to configure the sapphire transducer with the minimum possible power which maintains the effect of the amplifier noise temperature to the same order as the pump oscillator phase noise, this turns out to be about 0.05 mW.

Assuming the discussed operating conditions, the broad-band displacement noise due to the amplifier noise temperature and oscillator phase noise are compared in tables 1 and 2. It should be pointed out that if one is to compare transducers of different mass, it is necessary to calculate the effective displacement noise with respect to the vibrations of the primary bar mass by multiplying the displacement noise given by (7) and (8) by the square root of the mass ratio, $\mu = \sqrt{m_2/m_1}$. For the sapphire transducer and re-entrant cavity the mass ratio, μ, is 0.0068 and 0.024 respectively.

It is apparent that the re-entrant cavity is limited by the amplifier noise temperature. To improve this technology, an enhancement in the electrical Q and power handling capability is required. After many years at UWA no reliable enhancement of these parameters has been achieved. Conversely the sapphire transducer is limited by the oscillator phase noise and df/dx, even at an operating powers well below its power handling capability. From previous modelling, the df/dx could be raised as high as 8-9$\times 10^{12}$ Hz/m.[16] Based on these results it is apparent from table 1 and 2, that a lower broad-band noise floor of order 20 dB is attainable with a sapphire transducer.

Table 1: Broad band noise assuming T_{amp}=2.6×10^4 K and S_{pm}=-140 dBc/Hz.

	$\mu\sqrt{S_{RO}}$ due to T_{amp} [m/$\sqrt{Hz}$]	$\mu\sqrt{S_x}$ due to S_{pm} [m/$\sqrt{Hz}$]
Sapph. Trans.	4.5×10^{-20}	6×10^{-20}
Re-ent. Cav.	7.2×10^{-19}	6×10^{-21}

Table 2: Broad band noise assuming T_{amp}=8 K and S_{pm}=-180 dBc/Hz.

	$\mu\sqrt{S_{RO}}$ due to T_{amp} [m/$\sqrt{Hz}$]	$\mu\sqrt{S_x}$ due to S_{pm} [m/$\sqrt{Hz}$]
Sapph. Trans.	7.9×10^{-22}	6×10^{-22}
Re-ent. Cav.	1.3×10^{-20}	6×10^{-23}

8. Comparison of the Dielectric and Re-entrant Transducers at 15 mK

Cooling a parametric transducer to ultra cryogenic temperatures poses some further technical problems that must be overcome. Common problems for other ultra-cryogenic detectors operating with a SQUID include; operating with necessarily higher levels of vibration isolation cooled to ultra-cryogenic temperatures, and; supplying enough cooling power to cool massive objects of order 100 tonne. Specific to a parametric transducer, the dissipated pump power must be sufficiently low to allow cooling. However, if this can be overcome, a microwave transducer allows non-contacting coupling which may offer a significant advantage with regards to the vibration isolation problem.

It has been estimated that the restriction to the overall dissipated power is on the order of a μW,[19] this reduction in power will increase the contribution of the low noise microwave amplifier in the readout system, but at the same time reduce the effect of back-action due to the pump oscillator AM noise. Thus, for an ultra-cryogenic detector it is more crucial to obtain low noise temperature amplifiers. Also, the reduction in back-action is necessary if one is to make use of the lower Nyquist noise due to the ultra-cryogenic temperatures.

The high electrical Q of the sapphire transducer means that the bandwidth of the transducer is smaller than the modulation frequency. It has been shown that if the frequency of the pump is offset from the transducer resonance by, Δf_{PUMP}=f_0-f_1, then the acoustic resonator will still significantly modulate the carrier.[20] However, at this offset most of the carrier signal will be reflected, and the power dissipation is given by;

$$P_{dis} = \frac{P_{inc}\,\Delta f_{PUMP}}{2\,f_1\,Q_e} \tag{9}$$

If Q_e is assumed to be 10^9 with an input power of 135 μW incident on six transducers of a sphere, then the dissipated power will be 0.8 μW, which is acceptable. Assuming S_{am} ≈-180 dBc/Hz and P_{inc} ≈135 μW, from (5) and (6) the back-action can be calculated to be of the same order as the Nyquist noise. The re-entrant cavity has a smaller Q-factor and this trick may not be used. Thus, a limit of 0.1 μW to P_{inc} must be set. This corresponds to 0.6 μW for six transducers on a sphere, and makes

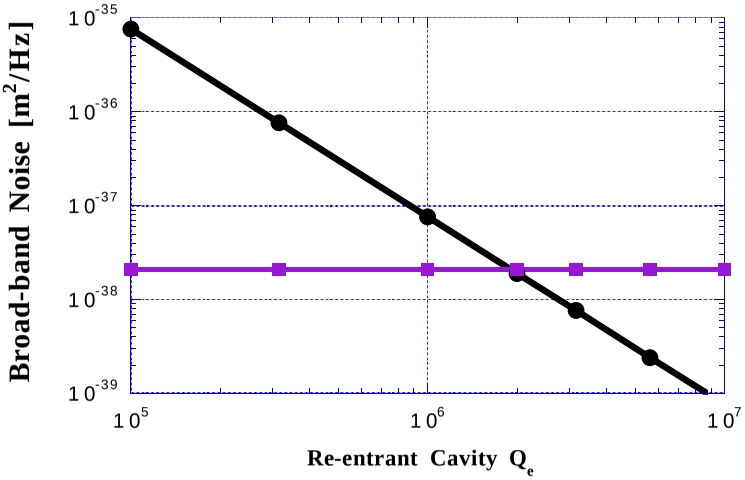

Figure 4: **Line with squares;** broad-band noise of the sapphire transducer. **Line with circles;** broad-band noise of the re-entrant cavity transducer as a function of electrical Q. If the re-entrant cavity improves to greater than 2×10^6 then it will be more sensitive than the sapphire transducer.

sure that the back-action noise due to S_{am} is below the Nyquist noise.

Cooling to ultra-cryogenic temperatures means that the sensitivity of the re-entrant cavity transducer is likely to improve due to an improvement in Q_e. No improvement will accompany the sapphire transducer if Q_e is increased, as its bandwidth is already smaller than the resonant-mass frequency. Figure 4 shows a comparison of the the broad-band noise with respect to a 0.035 kg final mass, assuming an amplifier noise temperature of 3 K, and a phase noise of -180 dBc/Hz. The dominant component of noise for both transducers is the amplifier noise temperature. For the sapphire transducer 1.4×10^{-38} is due to the amplifier and 7.8×10^{-39} is due to the pump phase noise.

9. Detector Sensitivity

Figure 5 shows the present and calculated spectral sensitivity of Niobe with expected improvements. Details of these calculations can be found in.[21] For the Grail sphere a study of the performance from 4 K to 15 mK for 2-5 mode systems was completed. The sapphire transducer was assumed to have an effective mass of m_n=0.035 kg, and the intermediate masses were assumed to be spread in mass geometrically, given that $m_1 > m_2 ..... > m_n$. It was assumed that all modes were made from CuAl with a Q-factor of 1.6×10^7,[22] except the last mode which was sapphire with a Q of 10^9.

At 4 K the Nyquist noise was large enough to limit the sensitivity to the order of 10^{-2} mK. At this temperature there is a distinct advantage in implementing a 4 to 5 mode system. At 15mK the sensitivity is limited by the transducer and thus there is not much difference between the 3 to 5 mode systems. A noise temperature

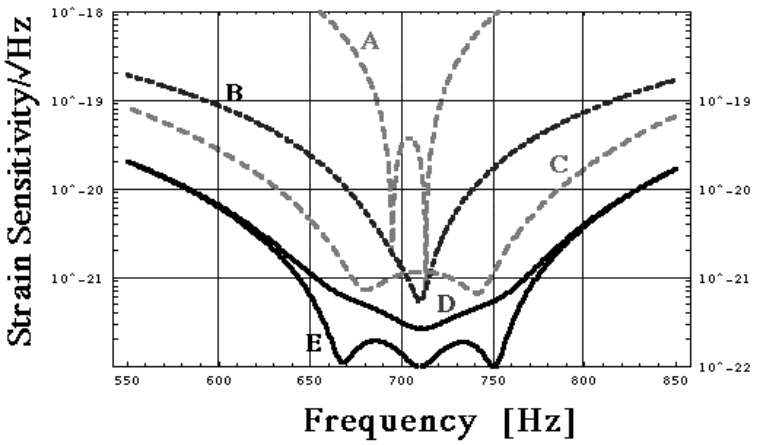

Figure 5: Strain Sensitivity/$\sqrt{Hz}$ versus frequency for Niobe. **Curve A** shows the current sensitivity. **Curve B** shows the expected improvement with a cryogenic HEMT microwave amplifier replacing the standard GaAs FET amplifier in the readout, and by improving the noise performance of the pump oscillator driving the transducer. **Curve C** show the sensitivity if we transform Niobe to a 3-mode detector with a re-entrant cavity transducer of mass of 0.035 kg. **Curve D** shows the projected performance of the 3-mode system with a sapphire transducer. The performance is not too far from the projected performance of the first stage LIGO detector which is about $10^{-22}/\sqrt{Hz}$ near 1 kHz. **Curve E** shows the performance of Niobe if it is cooled to the ultra-cryogenic temperature of 15mK.

of order 10^{-4} mK can be achieved which is very close to the quantum limit (0.5×10^{-4} mK). Even though at 15 mK there is not much difference between the integrated sensitivity given by (1), from figure 7 it is apparent that the spectral sensitivity is quite different. Thus, the choice of the number of modes could depend on the type of signal one expects to detect. The 3-mode system is more sensitive in a narrower band, so if one wants to detect a narrow band signal they might choose this configuration. As the number of modes increases the sensitivity is spread out to a larger frequency bandwidth.

10. Conclusion

At 4K it seems that the sapphire transducer may hold a significant advantage over the re-entrant cavity transducer. However, at 15 mK this will depend on how much the Q-factor of the re-entrant cavity will improve with cooling. We have shown that the sensitivity of a resonant-mass detector can approach the quantum limit using a parametric transducer and is worth further study. For NIOBE at 4 K, a millisecond burst sensitivity of order 10^{-20} can be achieved, corresponding to a spectral strain sensitivity of $2\times10^{-22}/\sqrt{Hz}$ with a 50 Hz bandwidth. This level of sensitivity is a factor of 25 in energy above the standard quantum limit. For the ultra-cryogenic spherical GRAIL detector in the Netherlands, a burst sensitivity of 4×10^{-22} can be achieved which corresponds to a spectral strain sensitivity of better than $10\times10^{-23}/\sqrt{Hz}$ with

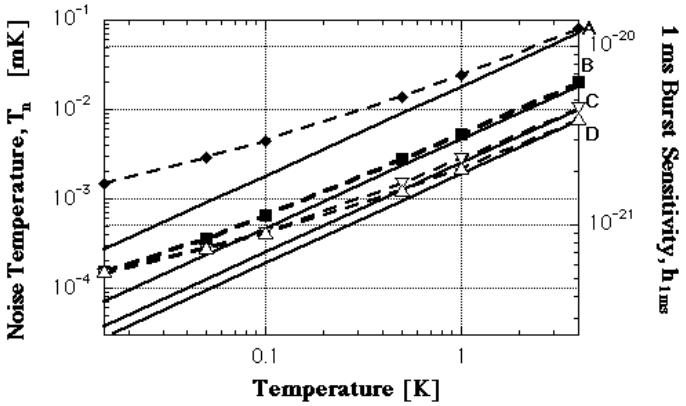

Figure 6: Grail sensitivity versus temperature from 4K to 15 mK. **Solid lines** represent the Nyquist limit and the **dashed curves** represent the Grail detector with a sapphire transducer. **Curve A** is a 2-mode system. **curve B** is a 3-mode system, **curve C** is a 4-mode system and **curve D** is a 5-mode system.

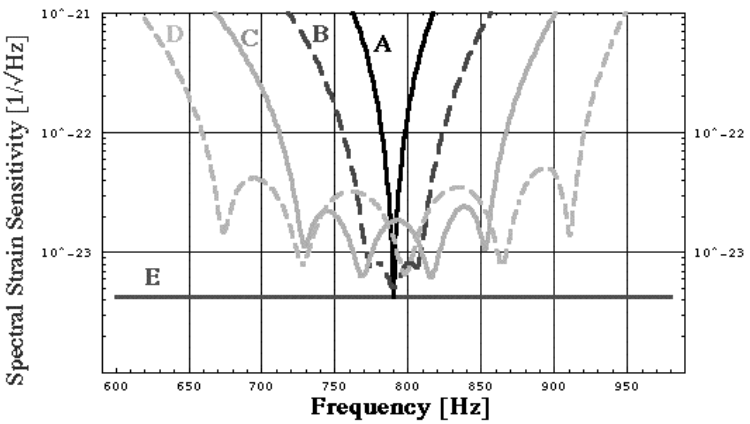

Figure 7: Calculated spectral strain sensitivity for the Grail detector with; **A,** 2-modes; **B,** 3-modes; **C,** 4-modes;**D,** 5-modes; **E,** an ideal noiseless transducer (Nyquist noise only due to primary mass).

a bandwidth of order 100 Hz, and is close to the quantum limit.

11. Acknowledgements

The author would like to thank Drs. Stevenson and Merkowitz for improving the authors understanding of a spherical detector, Prof. Frossati at the University of Leiden and the Grail team at NIKHEF for useful discussions and providing incentive to model the Grail detector. Also, he would like to thank the UWA group especially Dr. Ivanov and Prof. Blair for useful discussions. This work was supported by the Australian Research Council.

References

1. D. G. Blair, E. N. Ivanov, M. E. Tobar, P. J. Turner, F. V. Kann, and I. S. Heng, Phys. Rev. Let. **74,** 1908-1911 (1995).
2. H. Peng, D. G. Blair, and E. N. Ivanov, J. Phys. D: Applied Physics **27,** 1150 (1994).
3. B. D. Cuthbertson, M. E. Tobar, E. N. Ivanov, and D. G. Blair, Rev. of Sci. Inst. **67,** 2435-2442 (1996).
4. M. E. Tobar, E. N. Ivanov, D. K. L. Oi, B. D. Cuthbertson, and D. G. Blair, Appl. Phys. B **64,** 153-166 (1997).
5. R.A. Woode, M.E. Tobar, E.N. Ivanov, and D.G. Blair, IEEE Trans. on UFFC, **43(5),** (1996)
6. M. E. Tobar and D. G. Blair, IEEE Trans. on MTT **42,** 344-347 (1994).
7. M.E. Tobar, E.N. Ivanov, R.A. Woode, J.H. Searls, and A.G. Mann, IEEE MWGL **5,** 108-110 (1995).
8. E. N. Ivanov, M. E. Tobar, and R. A. Woode, IEEE MWGL **6,** 312-314 (1996).
9. V. B. Braginsky, V. P. Mitrofanov, and V. I. Panov, *Systems with small dissipation* (University of Chicago Press, 1985).
10. L. A. Wainstein and V. D. Zubakov, *Extraction of signals from noise (Prentice Hall*, Englewood Cliffs, NJ., 1962).
11. P. F. Michelson and R. C. Taber, J. Appl. Phys. **52,** 4313 (1981).
12. M. E. Tobar and D. G. Blair, Rev. of Sci. Instrum.**66,** 108-110 (1995).
13. C. Z. Zhou and P. F. Michelson, Phys. Rev. D **51,** 2517-2545 (1995).
14. T. R. Stevenson, Phys. Rev. D**56,** 564-587 (1997).
15. E. N. Ivanov, M. E. Tobar, and R. A. Woode, to be published in IEEE Trans. on MTT (1998).
16. B. D. Cuthbertson, M. E. Tobar, E. N. Ivanov, and D. G. Blair, to be published in IEEE Trans. on UFFC(1998).
17. A. N. Luiten, A. G. Mann, and D. G. Blair, IEE Electron. Let. **29,** 879-881 (1993).
18. E. N. Ivanov, M. E. Tobar, P. J. Turner, and D. G. Blair, rev. Sci. Instrum.**64,** 1905 (1993).

19. D. v. Albada, J. Flokstra, G. Frossati, E. P. J. v. d. Heuvel, J. W. v. Holten, A. T. A. M. d. Waele, and P. K. A. d. Witt-Huberts, Grail R and D Proposal, (1997).
20. M. E. Tobar and D. G. Blair, J. Phys. D: Applied Physics **26,** 2276-2291 (1993).
21. M. E. Tobar, E. N. Ivanov, and D. G. Blair, submitted to Phys. Let. A (1998).
22. G. Frossati, in Proc. of the Omni Directional Workshop Sao Jose dos Campos, Bazil, 1996.